

height. Assuming a linear relationship between thickness and absorption, as well as assuming a direct relationship between absorption and emission, the fluorescence signal, measured by NSOM, is expected to increase by the same percentage. The increase in fluorescence between the tallest feature and the background signal of 13 kcps is 13 kcps. Although this is not the total emission from the sample, since we have less than unity collection efficiency and we have placed a beam splitter in the path of the collected signal, as shown in Figure 1, we can compare the fluorescence percentage increase with the thickness percentage increase. Our observed fluorescence difference, as recorded in the NSOM image, is 100%. This compares well to the percentage increase in topography.

In contrast to the spin-cast film, the drop-cast film in Figure 4C exhibits an increased fluorescence yield that is not correlated to topography. Although the shear force image indicates undulating surface topography throughout the film, regions of higher topography do not necessarily correspond to regions of increased fluorescence. Brighter regions in the shear force image are indicative of thicker regions in the irregular drop-cast film. For a sufficiently thin film, such as our 20 nm film, thicker regions would be expected to yield more fluorescence in a given area. In this case, the regions with the most fluorescence are not correlated with the highest regions in the topography image. As appears to be the case for the 10  $\mu\text{m}$  Alq<sub>3</sub> film, variations in fluorescence may be due to local variations in the molecular packing of the Alq<sub>3</sub> molecules in film. In addition to the variation in fluorescence and topography, drop-cast films exhibited rms surface roughness of approximately 5 nm, the largest surface topography variation among the three deposition methods.

We have examined a variety of Alq<sub>3</sub> films (vacuum-deposited, drop-cast, and spin-cast) with confocal, near-field and shear force microscopy. NSOM allows direct probing of 10–100 nm features in Alq<sub>3</sub> films unseen in previous experiments. We found the vacuum-deposited Alq<sub>3</sub> film to be the most homogeneous film, both in terms of topography and fluorescence. In contrast, the drop-cast film had both the most varied surface topography and fluorescence, while the spin-cast film had large topographical features that directly correlated to increased local fluorescence efficiency.

### Experimental

Glass coverslips (Fisher) were used as sample substrates. The slides were rinsed in acetone and flamed before use. Alq<sub>3</sub> powdered solids were used as received (Aldrich). Several samples were vacuum-deposited purified Alq<sub>3</sub> (Thompson Group, USC) thin films. The solids were placed in a baffled tungsten evaporating boat (R. D. Mathis) and sublimed at low pressures ( $\sim 10^{-6}$  torr). The samples were stored in air. For spin-cast films, a stock solution ( $3.0 \times 10^{-4}$  M) of Alq<sub>3</sub> in acetone was made. The glass substrate was fixed to the stage of a homemade spin coater as 10  $\mu\text{L}$  aliquots of the solution were dropped onto the center of spinning glass ( $\sim 3500$  rpm). In addition, several Alq<sub>3</sub> films were made by allowing a drop of the stock solution to dry on a glass slide (drop casting). For vacuum-deposited films, sample

thickness was determined by a quartz crystal thickness monitor. Spin-cast and drop-cast film thicknesses were determined by profilometer (Sloan Dektak II).

Received: September 9, 1999

- [1] J. R. Sheats, H. Antoniadis, M. Hueschen, W. Leonard, J. Miller, R. Moon, D. Roitman, A. Stocking, *Science* **1996**, *273*, 884.
- [2] H. Aziz, Z. D. Popovic, N.-X. Hu, A.-M. Hor, G. Xu, *Science* **1999**, *283*, 1900.
- [3] A. Curioni, M. Boero, W. Andreoni, *Chem. Phys. Lett.* **1998**, *294*, 263.
- [4] C. W. Tang, S. A. VanSlyke, *Appl. Phys. Lett.* **1987**, *51*, 913.
- [5] G. E. Jabbour, S. E. S. Y. Kawabe, J. F. Wang, M. M. Morrell, B. Kippelen, N. Peyghambarian, *Appl. Phys. Lett.* **1997**, *71*, 1762.
- [6] M. Fujihira, L.-M. Do, A. Koike, E.-M. Han, *Appl. Phys. Lett.* **1996**, *68*, 1787.
- [7] F. Papadimitrakopoulos, X. M. Zhang, D. L. Thomsen, K. A. Higginson, *Chem. Mater.* **1996**, *8*, 1363.
- [8] A. D. Walser, I. Sokolik, R. Priestley, R. Dorsinville, *Synth. Met.* **1997**, *84*, 877.
- [9] K. Yase, S.-S. Sumimoto, H. Matsuda, M. Kato, *Mol. Cryst. Liq. Cryst.* **1995**, *267*, 151.
- [10] P. E. Burrows, Z. Shen, V. Bulovic, D. M. McCarty, S. R. Forrest, J. A. Cronin, M. E. Thompson, *J. Appl. Phys.* **1996**, *79*, 7991.
- [11] E. Betzig, J. K. Trautman, T. D. Harris, J. S. Weiner, R. L. Kostelak, *Science* **1991**, *251*, 1468.
- [12] E. Betzig, P. L. Finn, J. S. Weiner, *Appl. Phys. Lett.* **1992**, *60*, 2484.
- [13] K. D. Weston, S. K. Buratto, *J. Phys. Chem. A* **1998**, *102*, 3635.
- [14] J. A. DeAro, K. D. Weston, S. K. Buratto, U. Lemmer, *Chem. Phys. Lett.* **1997**, *277*, 532.

## Two-Dimensional Crosslinked Nanoparticle Networks\*\*

By Shaowei Chen\*

Fabrication of ordered arrays of nanoelectrodes and nanoclusters have recently attracted extensive research interest, due to the fundamental and technological significance associated with these nanoscale architectures.<sup>[1–8]</sup> One of their most striking characteristics is the so-called quantum effect that arises from the nanosized dimensions of the materials, demonstrated by various unique properties that are vastly different from those of single molecules or the bulk phase.<sup>[9–11]</sup> As their diverse application potentials are largely limited to the availability of methodologies for the fabrication of organized assemblies in a controllable fashion, a great deal of research effort has been focused on the development of different approaches.

Among the materials studied, monolayer-protected nanoclusters (MPCs)<sup>[12,13]</sup> emerged as a distinct member of the rapidly expanding family of advanced nanomaterials, which exhibit great stability in both solution and dry forms, in contrast to conventional colloidal particles. The development of new methods for the fabrication of their ordered ensembles might help pave the way towards their applications as the structural basis for electronic nanocircuits/

[\*] Prof. S. Chen  
Department of Chemistry and Biochemistry  
Southern Illinois University  
Carbondale, IL 62901-4409 (USA)

[\*\*] This work was supported by Southern Illinois University.

nanodevices, which are mainly ascribed to the sub-attofarad molecular capacitance associated with the dielectric protecting monolayer and the resulting single-electron charging characteristics.<sup>[14–16]</sup> There have been various approaches reported to immobilize MPCs onto substrate surfaces,<sup>[1–8,17–19]</sup> among which the Langmuir–Blodgett (LB) technique is a well-established technique for generating compact, ordered monolayers on the air/water interface,<sup>[1–6]</sup> which can then be used to construct solid-supported monolayer or multilayer structures. In addition, crosslinking of the particles can be facilitated by bifunctional linkers, which leads to significant enhancement of the lateral mechanical stability of the particle assembly as well as manipulation of materials properties such as optical and electronic characteristics. For instance, recently, 2D organized thin films of 2-aminoethanethiol-modified CdS semiconductor nanoparticles have been fabricated on the air/water interface using the crosslinking reagent glutaraldehyde in the subphase, where the deposited films demonstrated enhanced n-type photosensitivities.<sup>[20]</sup> However, for transition-metal nanoparticles, amino-terminated MPCs tend to form 3D insoluble aggregates upon removal of solvents. Therefore, to obtain stable 2D metal nanoparticle networks, a different approach should be adopted. Here we demonstrate an efficient method by taking advantage of the LB technique along with dithiols as bifunctional linkers on the water surface.

Dithiols have been previously used as linkers to obtain 3D crosslinked gold particle aggregates by introducing the dithiol ligands into the particle protecting monolayers.<sup>[21]</sup> Upon removal of solvents, this assembling process occurs quickly, efficiently, and yet uncontrollably.<sup>[21]</sup> To use dithiols as the linkers to achieve a 2D crosslinked nanoparticle network, we brought the particles and the rigid dithiol linkers into contact on the air/water interface, where the crosslinking process was confined to the interfacial region and could be initiated at relatively high surface pressure, presumably due to ligand intercalation and surface place-exchange reactions.<sup>[22]</sup>

In a typical experiment, 25  $\mu\text{L}$  of ca. 0.08 mM 1-hexanethiolate-protected gold (C6Au) nanoparticles dissolved in hexane were slowly cast dropwise onto the air/water interface by a microliter syringe, followed by the spreading of typically 50  $\mu\text{L}$  of 2.4 mM 4,4'-thiobisbenzenethiol (TBBT,  $\text{HS-C}_6\text{H}_4\text{-S-C}_6\text{H}_4\text{-SH}$ ) in  $\text{CHCl}_3$  (the molar ratio of C6:TBBT  $\approx$  1). The surface pressure–area ( $\pi$ – $A$ ) isotherm exhibits quite a significant difference upon barrier compression. Figure 1 shows the isotherms for C6Au particles before (a) and after (b,c) the introduction of TBBT. Without TBBT on the air/water interface (Fig. 1a), the surface pressure of the C6Au particle monolayer starts to increase at ca. 200  $\text{cm}^2$ , corresponding to an average particle area of 16.6  $\text{nm}^2$ , which is greater than the geometrical cross-sectional area of a single particle ( $\sim$  8.0  $\text{nm}^2$ , assuming the monolayer chains are fully extended; hence, the average MPC diameter is ca. 3.2 nm. For more details see the Ex-

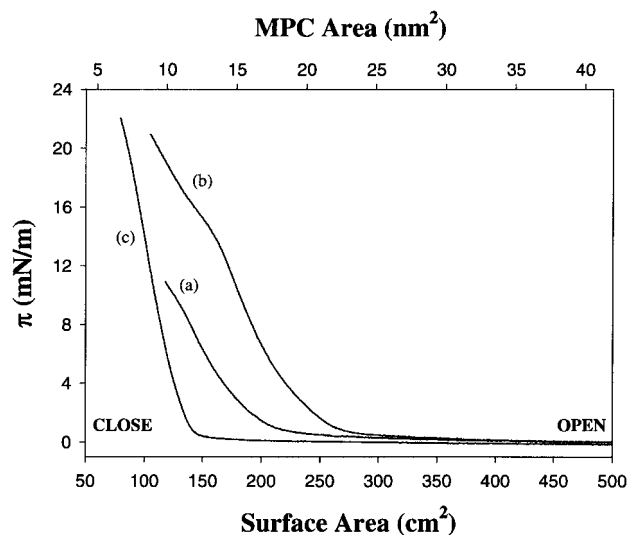


Fig. 1. Surface pressure ( $\pi$ ) and area ( $A$ ) isotherms of C6Au particles on the air/water interface in the absence (a) and presence (b,c) of dithiol linkers (TBBT): a) 25  $\mu\text{L}$  of ca. 0.08 mM C6Au solution in hexane; b,c) 50  $\mu\text{L}$  of 2.4 mM TBBT solution in  $\text{CHCl}_3$  were spread onto the water surface. Shown are the isotherms of the first compression (b) after the introduction of TBBT and when the crosslinking process was completed (c).

perimental section). At  $A < 200 \text{ cm}^2$  the gradual increase of surface pressure could be related to the formation of close-packed particle structures where monolayer–ligand intercalation would be possible at high surface pressure, akin to solid-state structure.<sup>[13]</sup> It should be noted that a collapse of the MPC monolayer did not appear to occur, and the isotherm was reproducible after repeated release–compression cycles.

Upon introduction of TBBT onto the interface, in the first compression (Fig. 1b), the surface pressure started to increase at a much larger surface area (260  $\text{cm}^2$ ), and the rising slope of the isotherm appeared to be very close to that without TBBT (a). However, after the barrier was held in the “closed” position (80  $\text{cm}^2$ ) for about 6 h, the isotherm generated from the subsequent compressions showed a strikingly different character (Fig. 1c): i) the surface pressure started to increase at an area even smaller than that in the absence of TBBT (Fig. 1a); ii) the gradient of the rising slope was much greater. (Note that 6 h is the time required to complete the crosslinking process and this time varied depending on the relative concentrations of the linker and the MPC molecules as well as surface pressure). More interestingly, on the water surface, macroscopic brown patches of particles (area on the order of 1  $\text{cm}^2$ ) were visible even when the barrier was moved back to the “open” position (500  $\text{cm}^2$ ). It should be mentioned that the particle patches appeared to be very stable for days. These observations strongly suggest the formation of a 2D cross-linked particle network. In a control experiment where no TBBT was added, no particle aggregates on the water surface could be visible when the barrier was moved to the “open” position even after the barrier was held in the “closed” position for 12 h, and the isotherms obtained thereafter were reproducible (Fig. 1a).

This crosslinking process is most likely to be initiated at high surface pressures where the monolayer structure is close to the so-called liquid-condense/solid phase. Intercalation of TBBT into the protecting monolayers of neighboring particles becomes possible, akin to the case of nanoparticles in the solid state, where surface-exchange reactions<sup>[22]</sup> can then occur, resulting in the crosslinking of neighboring particle molecules. As the particles used here were only partially fractionated, the crosslinking would most likely start with larger particles, which then helped sustain the network structures (see discussions below in the transmission electron microscopy (TEM) study).

The above particle assemblies were then deposited onto a cleaned glass slide surface by the LB dipping/lifting technique at a surface pressure  $\pi = 13$  mN/m, with two layers on the slide surface. The slide was then transferred to a UV-vis spectrometer for optical measurements. It is well-known that the distinct color of nanosized gold particles arises from the so-called surface plasmon (SP) resonance of Au 5d electrons, which superimposes onto the exponential-decay Mie scattering profile.<sup>[23-25]</sup> The energy of the SP band has been found to be sensitive to various factors, including particle size, shape, surrounding media, and interparticle interactions.<sup>[23-25]</sup> For alkanethiolate-protected gold nanoparticles smaller than 20 nm, the SP band was typically found at 520 nm.<sup>[13]</sup> Figure 2 shows the optical spectra of the C6Au particle solution and the deposited

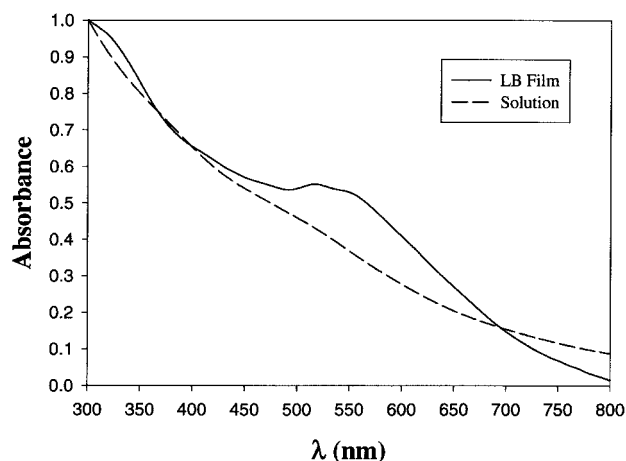


Fig. 2. Optical spectra of C6Au particles in hexane solution and deposited onto a glass slide by the LB method (two layers on both sides). The spectra were background-corrected and normalized to their respective absorbance at 300 nm.

particle films, both of which were background-corrected and normalized to their respective absorbance at 300 nm. One can see that, for the particles in hexane solution, a weak and broad SP band can be found at 520 nm, as expected, whereas for the LB film, the SP band (550 nm) is much more intense and shows a significant red-shift (30 nm).<sup>[26]</sup> This is consistent with the networking of the particle molecules, where the red-shift of the SP energy is attributed to the electronic coupling interactions between neighboring particles,<sup>[27,28]</sup> akin to the case where gold col-

loidal particles were brought close to each other by complementary oligonucleotide chains.<sup>[28]</sup>

The particle network structure was then studied by TEM. To demonstrate the stability of the particle patches, here a rather “low-tech” procedure was adopted where the sample was prepared by tweezers holding a Formvar-coated copper grid and the deposition of particles was effected by lifting the grid from underneath the particle patch. It should be noted that this was performed when the barrier was in the “open” position. From the TEM micrograph (Fig. 3), one can see that close-packed particle structure was achieved, though not all particles appeared to be

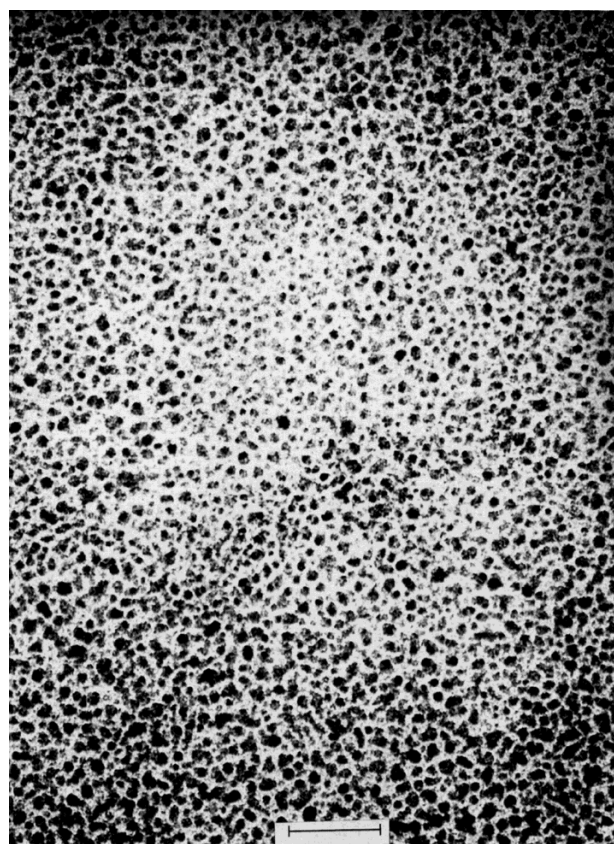


Fig. 3. Transmission electron micrograph of the gold particle patches obtained in Figure 1c. Scale bar 33 nm.

linked to one another as the interparticle distance was more than a single TBBT molecular length (presumably, the interparticle space was filled up by excess TBBT and displaced C6 molecules). However, no long-range regular superlattice structure was found here, in part, because the particles were only partially fractionated with modest size dispersity (20 %) and of non-uniform shape, and because the dithiol linkage was relatively strong so that molecular adjustment was impeded. Also, one can see that particles of varied core sizes were mixed rather randomly, instead of forming distinct domain structures. In addition, in the well-knitted region, the closest edge-to-edge distance between neighboring particles appeared to be about 1.0 nm, roughly equal to that of the TBBT molecular length.

Similar networking structures were also obtained with gold particles where multiple copies of dithiols were exchanged into the protecting monolayers prior to LB compression, as well as with other metal particles such as alkanethiolate-protected palladium particles.<sup>[29]</sup> By using the air/water interface as the substrate, networking structures of metal as well as semiconductor nanoparticles can, in principle, be constructed by the above approach with appropriate bifunctional linkers. With monodisperse particles, it is likely that a macroscopic superlattice network can be fabricated, where the particle distribution can be manipulated by, for instance, the linker chain length. The resulting assemblies can then easily be deposited onto solid substrate surfaces and serve as the structural basis for the construction of more complicated nanocomposite structures, on which further investigations can be carried out, for instance, anisotropic electron-transfer (hopping) kinetics, optoelectronic properties, and nanoparticle-based lithography.<sup>[30]</sup>

To conclude, 2D crosslinked nanoparticle networks were fabricated by the Langmuir–Blodgett technique where the bridging of neighboring particles was effected by rigid dithiol linkers, resulting in macroscopic patches of particles visible on the air/water interface even at low surface pressure. TEM measurements revealed close-packed particle assemblies, consistent with the red-shift observed in the optical spectroscopy measurements.

## Experimental

1-Hexanethiolate-protected gold (C6Au) nanoparticles were synthesized in a biphasic system, as reported previously [12,13]. The particles were then partially fractionated using a mixture of toluene and ethanol [31], with the final gold cores consisting of roughly 145 gold atoms (average core diameter 1.6 nm) [13]. 4,4'-Thiobisbenzenethiol (from Aldrich) and all solvents were used as received. LB studies were conducted at room temperature on a Nima 611D Langmuir–Blodgett trough with a Welhelmy plate as the surface-pressure sensor and nanopure water (supplied by a Barnstead Nanopure water system, 18.3 M $\Omega$ ) as the subphase. A solution (0.08 mM) of the fractionated particles was prepared in hexane while TBBT was dissolved in chloroform to make a concentration of ca. 2.4 mM. The calculated amount of the solutions was cast dropwise onto the water surface using a Hamilton microliter syringe. At least 20 min was allowed for evaporation prior to isotherm measurement and between compressions. Two particle layers were deposited onto both sides of a cleaned glass slide at a surface pressure  $\pi = 13$  mN/m. Optical measurements were carried out with a Unicam ATI UV-4 spectrometer with a resolution of 2 nm. The surface-plasmon band positions were determined by the second-order derivatives of the spectra. The TEM study was carried out with a Hitachi H7100 microscope (75 keV). Typically phase-contrast micro-images were captured at 300 K to 400 K magnification.

Received: July 20, 1999

Final version: September 8, 1999

- [1] M. Burghard, G. Philipp, S. Roth, K. von Klitzing, R. Pugin, G. Schmid, *Adv. Mater.* **1998**, *10*, 842.
- [2] S.-R. Yeh, M. Seul, B. I. Shraiman, *Nature* **1997**, *386*, 57.
- [3] M. Trau, D. A. Saville, I. A. Aksay, *Science* **1996**, *272*, 706.
- [4] C. P. Collier, R. J. Saykally, J. J. Shiang, S. E. Henrichs, J. R. Heath, *Science* **1997**, *277*, 1978.
- [5] W.-Y. Lee, M. J. Hostetler, R. W. Murray, M. Majda, *Isr. J. Chem.* **1997**, *37*, 213.
- [6] K. C. Yi, Z. Hórvölgyi, J. H. Fendler, *J. Phys. Chem.* **1994**, *98*, 3872.
- [7] M. Giersig, P. Mulvaney, *Langmuir* **1993**, *9*, 3408.
- [8] Z. L. Wang, *Adv. Mater.* **1998**, *10*, 13.

- [9] G. Schmid, *Clusters and Colloids: From Theory to Applications*, VCH, Weinheim, Germany **1994**.
- [10] H. Haberland, *Clusters of Atoms and Molecules*, Springer, New York **1994**.
- [11] M. A. Hayat, *Colloidal Gold: Principles, Methods and Applications*, Academic Press, New York **1989**, Vol. 1.
- [12] M. Brust, M. Walker, D. Bethell, D. J. Schiffrin, R. Kiely, *J. Chem. Soc., Chem. Commun.* **1994**, 801.
- [13] M. J. Hostetler, J. E. Wingate, C.-H. Zhong, J. E. Harris, R. W. Vachet, M. R. Clark, J. D. Londono, S. J. Green, J. J. Stokes, G. D. Wignall, G. L. Glish, M. D. Porter, N. D. Evans, R. W. Murray, *Langmuir* **1998**, *14*, 17.
- [14] S. Chen, R. S. Ingram, M. J. Hostetler, J. J. Pietron, R. W. Murray, T. G. Schaaff, J. T. Khoury, M. M. Alvarez, R. L. Whetten, *Science* **1998**, *280*, 2098.
- [15] R. S. Ingram, M. J. Hostetler, R. W. Murray, T. P. Bigioni, D. K. Guthrie, P. N. First, *J. Am. Chem. Soc.* **1997**, *119*, 9279.
- [16] S. Chen, R. W. Murray, S. W. Feldberg, *J. Phys. Chem. B* **1998**, *102*, 9898.
- [17] S. Chen, R. W. Murray, *J. Phys. Chem. B* **1999**, *103*, 9996.
- [18] M. Gao, B. Richter, S. Kristein, *Adv. Mater.* **1997**, *9*, 802.
- [19] C. B. Murray, C. R. Kagan, M. G. Bawendi, *Science* **1995**, *270*, 1335.
- [20] T. Torimoto, N. Tsumura, M. Miyake, M. Nishizawa, T. Sakata, H. Mori, H. Yoneyama, *Langmuir* **1999**, *15*, 1853.
- [21] M. Brust, D. Bethell, D. J. Schiffrin, C. J. Kiely, *Adv. Mater.* **1995**, *7*, 795.
- [22] M. J. Hostetler, A. C. Templeton, R. W. Murray, *Langmuir* **1999**, *15*, 3782.
- [23] M. Kerker, *The Scattering of Light and Other Electromagnetic Radiation*, Academic Press, New York **1969**.
- [24] C. F. Bohren, D. R. Huffmann, *Absorption and Scattering of Light by Small Particles*, Wiley, New York **1983**, Ch. 12.
- [25] S. Underwood, P. Mulvaney, *Langmuir* **1994**, *10*, 3427.
- [26] The appearance of a second absorption peak (at ca. 516 nm, Fig. 2) in the optical measurement was caused by data smoothing with Peakfit.
- [27] M. P. Pileni, *New J. Chem.* **1998**, 693.
- [28] C. A. Mirkin, R. L. Letsinger, R. C. Mucic, J. J. Storhoff, *Nature* **1996**, *382*, 607.
- [29] S. Chen, K. Huang, J. A. Stearns, *Chem. Mater.*, in press.
- [30] C. P. Collier, T. Vossmeier, J. R. Heath, *Annu. Rev. Phys. Chem.* **1998**, *49*, 371.
- [31] T. G. Schaaff, M. N. Shafiqullin, J. T. Khoury, I. Vezmar, R. L. Whetten, W. G. Cullen, P. N. First, C. Gutiérrez-Wing, J. Ascencio, M. J. Jose-Yacamán, *J. Phys. Chem. B* **1997**, *101*, 7885.

## Trapping Light in Polymer Photodiodes with Soft Embossed Gratings\*\*

By Lucimara Stolz Roman,\* Olle Inganäs,\*  
Thomas Granlund, Tobias Nyberg, Mattias Svensson,  
Mats R. Andersson, and Jan C. Hummelen

Conjugated polymers are an attractive choice for use in electronic devices. Polymeric transistors,<sup>[1]</sup> light-emitting

- [\*] L. S. Roman, Dr. O. Inganäs, T. Granlund, T. Nyberg  
Laboratory of Applied Physics, Department of Physics (IFM)  
Linköping University  
SE-581 83 Linköping (Sweden)  
M. Svensson, Dr. M. R. Andersson  
Department of Polymer Technology  
Chalmers University of Technology  
SE-41296, Göteborg (Sweden)  
Dr. J. C. Hummelen  
Stratingh Institute & MSC, University of Groningen  
Nijenborgh 4, NL-9747 AG Groningen (The Netherlands)

[\*\*] The authors acknowledge the financial support of the Göran Gustafsson foundation Sweden and thank L. A. A. Pettersson for valuable discussions.